Journal of Engineering Mathematics, Vol. 15, No. 1, January 1981

High Reynolds number flows with closed streamlines

N. RILEY

School of Mathematics and Physics, University of East Anglia, Norwich, England.

(Received January 2, 1980)

SUMMARY

In this paper we consider high Reynolds number flows with closed streamliness within which an inviscid region of uniform vorticity is separated from the containing boundary by viscous boundary layers. From numerical solutions of the boundary-layer equations we are able to determine that value of the core vorticity for which inviscid core and boundary layer are compatible.

1. Introduction

Consider the steady, two-dimensional, laminar motion within a closed region which is induced by a given velocity distribution along the external boundary whose shape and orientation remain fixed. The resulting motion will be one in which the streamlines are closed, and if the Reynolds number is large there will be an inviscid core, within which the vorticity is uniform, separated from the moving boundary by viscous boundary layers. A proof of this result is given by Batchelor [1]. This overall picture of the flow is confirmed by numerical solutions of the Navier-Stokes equations at high Reynolds number, as for example the flow in a square cavity discussed by Burggraf [2]. The core vorticity, which is related to the motion of the boundary, can only be determined from a consideration of the boundary layer which separates the core flow from the boundary. For the special case in which the boundary is circular the core vorticity is determined from a simple integral of the boundary-layer equations (see [1]).

In this paper we consider, using numerical methods, the problem of determining the core vorticity for the general case in which the boundary is non-circular. We note that there will be one value of the core vorticity for which a steady solution of the boundary-layer equations is available. Following a study of the nature of the outer part of the boundary-layer solution, we demonstrate the form that the steady solution of the boundary-layer equations takes close to the *finite* outer boundary, which it is necessary to adopt in a numerical scheme, for any value of the core vorticity. From these considerations we formulate a criterion, based upon matching the boundary-layer and core vorticities, which enables us to determine that value of the core vorticity which is consistent with a steady solution of the boundary-layer equations. The criterion is not dissimilar to that in [3]. We apply these ideas to a class of flows in elliptical regions, and we compare the results obtained with the result derived from assuming that the streamlines are circular.

2. Flows with closed streamlines: the boundary layer

As we have noted in Section 1, in a high-Reynolds number steady flow with closed streamlines the vorticity is uniform in a region where viscous forces are small, and the value, say ω_0, of the vorticity is determined from a consideration of the boundary layers surrounding the core.

Consider a region S surrounded by a closed curve C which represents a solid boundary; all or part of the boundary is in steady motion, which typical speed U_0, and a fluid motion is induced within S. The shape and orientation of C remain unchanged. If d is a typical diameter of the region, see Fig. 1, then we assume that the Reynolds number $R = U_0 d/\nu$ is large, where ν is the kinematic viscosity of the fluid. We choose U_0, d as a typical velocity and length respectively so that U_0/d is the scale of the core vorticity. With respect to the boundary-layer co-ordinates (x,y) of Fig. 1, for which the corresponding velocity components are (u,v) (where an appropriate boundary-layer scaling with $R^{1/2}$ has been incorporated), the steady flow in the boundary layer is governed by the following equations and boundary conditions:

$$\frac{\partial u}{\partial x} + \frac{\partial v}{\partial y} = 0, \tag{2.1}$$

$$u\frac{\partial u}{\partial x} + v\frac{\partial u}{\partial y} = U_1\frac{dU_1}{dx} + \frac{d^2u}{\partial y^2}, \tag{2.2}$$

$$\begin{aligned} &u = U_s,\ v = 0 \text{ at } y = 0,\\ &u \to U_1 \text{ as } y \to \infty,\\ &u(x + 2l) = u(x). \end{aligned} \tag{2.3}$$

In these equations the velocity at the edge of the boundary-layer $U_1 = U_1(x;\omega_0)$ is determined from the inviscid core flow and depends upon the single parameter ω_0, $U_s = U_s(x)$ is the prescribed 'skin velocity' of the boundary and $2l$ is the length of the bounding curve C.

In the especially simple case where the bounding curve C is a circle, so that the inviscid core is a solid-body rotation with circular streamlines, the pressure-gradient term in (2.2) is identically zero and there is a simple relationship between U_s and U_1 (see [1]), namely

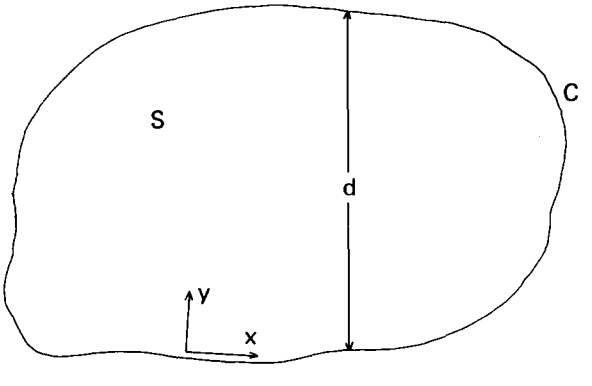

Figure 1. The geometry and co-ordinate system.

$$\int_0^{2l} U_s^2\, dx = \int_0^{2l} U_1^2\, dx, \tag{2.4}$$

from which, since $U_1 = \tfrac{1}{2}\omega_0$, we have

$$\omega_0 = \left(\frac{2}{l}\int_0^{2l} U_s^2\, dx\right)^{\frac{1}{2}}. \tag{2.5}$$

The result (2.4) is determined by first introducing a new independent variable ψ into (2.2), where ψ is the stream function, and integrating around a closed streamline. This process yields a simple differential equation from which we have

$$\int_0^{2l} u^2\, dx = \text{const.} \tag{2.6}$$

The argument which leads to (2.6) fails in the more general case due to the presence of the pressure-gradient term in (2.2).

It is instructive, for what follows, to consider in more detail the particularly simple case where the skin velocity on the circular boundary has only a small variation from a uniform value, so that to first order fluid and containing boundary are in rigid-body rotation.
Thus we write

$$\begin{aligned} U_s &= 1 + \epsilon f(x) + O(\epsilon^2), \\ U_1 &= 1 + \epsilon \tilde{\omega}_0 + O(\epsilon^2), \end{aligned} \tag{2.7}$$

where $f(x)$ is a prescribed periodic function with period $2l = 2\pi$, $\tilde{\omega}_0$ is a constant to be determined, and $\epsilon \ll 1$. Since $f(x)$ is periodic, with period 2π, we may write

$$f(x) = \frac{1}{2} a_0 + \sum_{n=1}^{\infty} (a_n \cos nx + b_n \sin nx),$$

where

$$a_n = \frac{1}{\pi}\int_0^{2\pi} f(x)\cos nx\, dx,\ b_n = \frac{1}{\pi}\int_0^{2\pi} f(x)\sin nx\, dx,\quad n = 0, 1, 2 \ldots . \tag{2.8}$$

We now write

$$\begin{aligned} u &= 1 + \epsilon \tilde{u} + O(\epsilon^2), \\ v &= \epsilon \tilde{v} + O(\epsilon^2), \end{aligned} \tag{2.9}$$

and from the linearized form of (2.2) we determine the solution for $\tilde{u}$ as

$$\tilde{u} = \frac{1}{2}(a_0 + \Omega_0 y) + \sum_{n=1}^{\infty} e^{-ny/\sqrt{2}} \left\{ (a_n \cos nx + b_n \sin nx) \cos \frac{ny}{\sqrt{2}} + \right.$$
$$\left. + (nb_n \cos nx + n^{-1} a_n \sin nx) \sin \frac{ny}{\sqrt{2}} \right\}, \tag{2.10}$$

where the conditions at $y = 0$, and the periodicity condition have been satisfied but not, at this stage, the condition as $y \to \infty$. Consider, in general, conditions as $y \to \infty$. The vorticity in the core is an $O(1)$ quantity whilst the vorticity in the boundary layer is $O(R^{1/2})$. In order that the vorticity matches satisfactorily we require $\partial u/\partial y \to 0$ as $y \to \infty$, and applying this condition to (2.10) gives $\Omega_0 \equiv 0$. Finally, applying the condition that $\tilde{u} \to \tilde{\omega}_0$ as $y \to \infty$ gives

$$\tilde{\omega}_0 = \frac{1}{2} a_0 = \frac{1}{2\pi} \int_0^{2\pi} f(x) dx, \tag{2.11}$$

which is in accord with the result (2.4).

Now in a numerical solution of the boundary-layer equations, and we discuss such a solution below, it will be necessary to prescribe $\tilde{\omega}_0$ and transfer the outer boundary condition to some remote, but finite, point $y = y_\infty$. We then see that a steady periodic solution of the form (2.10) is available provided that we choose

$$\Omega_0 = \left. \frac{\partial \tilde{u}}{\partial y} \right|_{y=y_\infty} = \frac{2\tilde{\omega}_0 - a_0}{y_\infty} . \tag{2.12}$$

Although Ω_0 chosen in this way in incorrect we may, by choosing y_∞ to be sufficiently large in our numerical procedure, be unaware of this fact.

Bearing the above considerations in mind we next address ourselves to the general problem in which the pressure gradient in (2.2) is non-zero. We examine conditions at the edge of the boundary layer by writing, as $y \to \infty$,

$$u = U_1 + \tilde{u}, \quad v = -y U_1' + \tilde{v},$$
$$\text{where} \quad |\tilde{u}|, |\tilde{v}_y| \ll U_1 . \tag{2.13}$$

We suppose that ω_0, and hence U_1, are known exactly and since U_1 is periodic we have

$$U_1 = \frac{1}{2} \alpha_0 + \sum_{n=1}^{\infty} \left(\alpha_n \cos \frac{n\pi x}{l} + \beta_n \sin \frac{n\pi x}{l} \right),$$

$$\alpha_n = \frac{1}{l} \int_0^{2l} U_1 \cos \frac{n\pi x}{l} \, dx, \quad \beta_n = \frac{1}{l} \int_0^{2l} U_1 \sin \frac{n\pi x}{l} \, dx, \quad n = 0, 1 \ldots . \tag{2.14}$$

Substituting (2.13) into (2.1), (2.2) gives the following linear equation for $\tilde{u}$:

$$\tilde{u}\frac{dU_1}{dx} + U_1\frac{\partial\tilde{u}}{\partial x} - y\frac{dU_1}{dx}\frac{\partial\tilde{u}}{\partial y} = \frac{\partial^2\tilde{u}}{\partial y^2}\,, \tag{2.15}$$

which is simplified by writing $\phi = \tilde{u}U_1$, $z = yU_1$ to

$$\frac{\partial\phi}{\partial x} = U_1\frac{\partial^2\phi}{\partial z^2}\,. \tag{2.16}$$

A separable solution $\phi = X(x)Z(z)$ of (2.16) which satisfies the condition $\tilde{u}\to 0$ as $y\to\infty$ is given by

$$X = \exp(i\lambda^2\int U_1 dx),\quad Z = A\exp\{-\frac{(1+i)}{\sqrt{2}}\lambda z\}, \tag{2.17}$$

where λ^2 is the separation constant and A a constant of integration. The periodicity of ϕ and hence $\tilde{u}$ is ensured if we choose

$$\lambda = \lambda_n = \left(\frac{2n\pi}{\alpha_0 l}\right)^{1/2}, \tag{2.18}$$

so that finally, as $y\to\infty$,

$$\tilde{u} = U_1^{-1}\sum_{n=1}^{\infty} A_n \exp\left\{\frac{2n\pi i}{\alpha_0 l}\int U_1 dx - (1+i)\left(\frac{n\pi}{\alpha_0 l}\right)^{1/2} y\,U_1\right\}. \tag{2.19}$$

There are several features of (2.19), which shows how a periodic boundary layer approaches the free-stream velocity, which are worthy of further comment. Firstly we note from the complex exponent that the free-stream velocity is not approached monotonically but through decaying oscillations. Secondly we see that although the decay to the free-stream velocity is exponential it is not as fast as the decay rate for non-periodic boundary layers which involve the exponential of the square of the distance from the boundary. Finally, from the factor U_1 in the exponent, we infer that the penetration distance of the boundary layer increases as the free-stream speed decreases. All the above features have been observed in the numerical solutions which we describe below.

The solution (2.19) matches satisfactorily in all respects with the inviscid core solution, as it should since we have assumed that ω_0 and hence U_1 is correctly given. Suppose now that ω_0 is changed by a small amount, $O(\epsilon)$, so that we require $\tilde{u}\to\epsilon U_1$ as $y\to\infty$. There can now be no steady solution of our boundary-layer equations since the core vorticity is given incorrectly. We might then enquire about the form which $\tilde{u}$ will take if we seek an approximate solution by numerical methods, when the condition as $y\to\infty$ is replaced by one at $y = y_\infty$. As before we write u, v as in equation (2.13), and find that $\tilde{u}$ satisfies (2.15) with the extra term $2\epsilon U_1 dU_1/dx$ on the right-hand side. It is tempting to simply add ϵU_1 to (2.19), but this cannot be correct since we would then have found the asymptotic form of a solution which matches with the inviscid core for another value of the core vorticity. There will be no such steady solution. However if we apply the outer condition at $y = y_\infty$ then we may anticipate, from the simple problem discussed above, that

$$\tilde{u} = \epsilon\left\{U_1 + A(x)\left(\frac{y-y_\infty}{y_\infty}\right) + B(x)\left(\frac{y-y_\infty}{y_\infty}\right)^2 + \ldots\right\} + \tilde{u}\,(\text{exp}), \tag{2.20}$$

where $\tilde{u}$ (exp) is as given in (2.19). If we substitute (2.20) into the equation for $\tilde{u}$ we find that the periodic functions $A(x)$, $B(x)$ etc. are simply related with $A(x)$ itself determined from the global boundary-layer calculation. The form of solution (2.20) gives $\partial\tilde{u}/\partial y = \epsilon A(x)/y_\infty$ at $y = y_\infty$ which, for fixed ϵ, decreases as y_∞ increases.

The above considerations allow us to formulate a criterion which enables us to distinguish, from amongst the steady periodic boundary-layer solutions which we obtain numerically, that which matches satisfactorily with the inviscid core and so allows us to determine the core vorticity ω_0. In the next session we consider a particular example.

3. An example

We take the bounding curve C to be an ellipse with semi-major and -minor axes a and b respectively so that C is given by

$$\frac{X^2}{a^2} + \frac{Y^2}{b^2} = 1. \tag{3.1}$$

We introduce elliptic co-ordinates (ξ, η) related to the rectangular co-ordinates (X, Y) by

$$X = 2e^{-\eta_0} \cosh\eta \cos\xi, \quad Y = 2e^{-\eta_0} \sinh\eta \sin\xi, \tag{3.2}$$

where $\eta = \eta_0$ is the ellipse C so that

$$a = 2e^{-\eta_0} \cosh\eta_0, \quad b = 2e^{-\eta_0} \sinh\eta_0, \tag{3.3}$$

and the eccentricity e of the ellipse is given by

$$e = \{1 - (b/a)^2\}^{1/2} = \operatorname{sech}\eta_0. \tag{3.4}$$

The scale factors associated with these co-ordinates are equal and are given by

$$h(\xi, \eta) = 2e^{-\eta_0} (\sinh^2\eta + \sin^2\xi)^{1/2}. \tag{3.5}$$

In the inviscid core, where the vorticity ω_0 is uniform, we solve Poisson's equation for the stream function ψ which in these co-ordinates is

$$\frac{\partial^2\psi}{\partial\xi^2} + \frac{\partial^2\psi}{\partial\eta^2} = -4\omega_0 e^{-2\eta_0} (\sinh^2\eta + \sin^2\xi), \tag{3.6}$$

whose solution, with $\psi = \text{const}$ on $\eta = \eta_0$, is

$$\psi = -2\omega_0 e^{-2\eta_0} \left(\frac{\sinh^2\eta_0 \cosh^2\eta \cos^2\xi + \cosh^2\eta_0 \sinh^2\eta \sin^2\xi}{\cosh^2\eta_0 + \sinh^2\eta_0} \right). \tag{3.7}$$

From (3.7) we may calculate the velocity at the edge of the boundary layer, U_1, as

$$U_1 = \frac{1}{h}\frac{\partial \psi}{\partial \eta}\bigg|_{\eta=\eta_0} = \omega_0 e^{-\eta_0} \tanh 2\eta_0 \,(\sinh^2 \eta_0 + \sin^2 \xi)^{1/2} . \tag{3.8}$$

With

$$\theta = \xi, \quad y = R^{1/2}(\eta_0 - \eta)h_0, \tag{3.9}$$

where $h_0 = h(\xi, \eta_0)$, the boundary-layer problem may be expressed as

$$\frac{1}{h_0}\frac{\partial u}{\partial \theta} + \frac{\partial v}{\partial y} = 0, \tag{3.10}$$

$$\frac{u}{h_0}\frac{\partial u}{\partial \theta} + v\frac{\partial u}{\partial y} = \frac{U_1}{h_0}\frac{dU_1}{d\theta} + \frac{\partial^2 u}{\partial y^2} , \tag{3.11}$$

with

$$\begin{aligned} &u = U_s, \quad v = 0 \quad \text{at} \quad y = 0, \\ &u \to U_1 \quad \text{as} \quad y \to \infty , \\ &u(\theta + 2\pi) = u(\theta), \end{aligned} \tag{3.12}$$

where $U_1 = U_1(\theta, \omega_0)$ is given by (3.8). For the skin velocity U_s we have taken, in all our calculations,

$$U_s = 1 + \frac{3}{4}\cos\theta . \tag{3.13}$$

This choice is arbitrary; we have avoided the classical 'sleeve' velocity (see [1]) on account of the singularity which is introduced into the boundary-layer solution at points where U_s is discontinuous.

The circle is, of course, a special case corresponding formally to $\eta_0 \to \infty$. In that case the exact result (2.5) is available, from which we deduce that

$$\omega_0 = 2.26385. \tag{3.14}$$

In the next section we discuss the numerical solution of the problem posed by equations (3.10) to (3.13).

4. Numerical results

The technique which we have employed to solve the equations (3.10) to (3.13) numerically is a fairly standard one and involves quasi-linearization of the first term on the left-hand side of (3.11), so that we write

$$u\frac{\partial u}{\partial \theta} \approx \bar{u}\frac{\partial u}{\partial \theta} + u\frac{\partial \bar{u}}{\partial \theta} - \bar{u}\frac{\partial \bar{u}}{\partial \theta} , \tag{4.1}$$

where, in the iterative solution at each station, an overbar denotes the value obtained from the previous iteration. In the iterative scheme we determine v from (3.10) by a simple quadrature and then using the Crank-Nicolson method, with derivatives replaced by central differences, we solve (3.11) for u and repeat the cycle until the difference between successive iterates falls below some prescribed tolerance. At that stage we advance to the next station. For a given value of ω_0, and hence U_1, we satisfy the periodicity condition in (3.12) by integrating over as many periods as is necessary for a periodic solution to emerge. For values of ω_0 which are different from the exact value a steady periodic solution is only available by virtue of the fact that we work on the finite interval $0 \leqslant y \leqslant y_\infty$, as we have discussed in Section 3. The starting profile for each value of ω_0 is either taken from the solution for the previous value or from

$$u = U_s + (U_1 - U_s)(1 - e^{-y}). \tag{4.2}$$

If the value of ω_0 was not changed by a large amount the former choice, in general, gave more rapid overall convergence. In most of the calculations described below we have taken step lengths $\delta\theta = \pi/30, \quad \delta y = 0.15$.

For our first example we have chosen the case of a circle, for which $e = 0$, by setting $\eta_0 = 20$ in the governing equations. For different values of y_∞ and a range of values of ω_0 we have obtained solutions in the manner described above. Since our aim is, essentially, to determine the solution for which $\epsilon = 0$ in (2.20) we have used $|\partial u/\partial y|_{y=y_\infty}$ as a measure of the closeness of our choice of ω_0 to the exact value. In Fig. 2 we show the integral of $|\partial u/\partial y|_{y=y_\infty}$ around C for different values of y_∞ and a range of values of ω_0. For each of the two cases shown we suggest that the minimum is close to the exact value of ω_0. That the integral is so relatively large at the minimum is accounted for by the fact that the values of y_∞ chosen are not sufficiently large for the exponential term in (2.19) to have decayed to zero. We have finally chosen $y_\infty = 18$ in all the calculations described. For the case of the circle we have repeated the calculations with

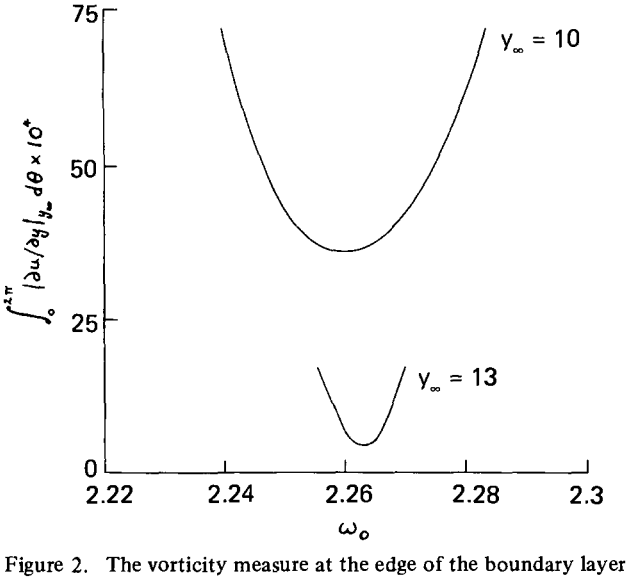

Figure 2. The vorticity measure at the edge of the boundary layer for the case $e = 0$.

a mesh size $\delta\theta = \pi/15$, $\delta y = 0.3$ and from the two estimates of ω_0 we have used h^2-extrapolation to determine a more accurate estimate of ω_0, namely

$$\omega_0 = 2.26378, \tag{4.3}$$

which may be compared with the exact value in (3.14). We have carried out similar calculations for different values of y_∞ in the case of an ellipse with $a/b = \sqrt{2}$, or $e = 0.71$. The results, in which the same measure as before has been used, are shown in Fig. 3. Exactly the same trends as for the case $e = 0$ are observed, with the minimum for each curve giving an approximation to the appropriate value of ω_0. Again the value of $y_\infty = 18$ yielded accurate results for this case.

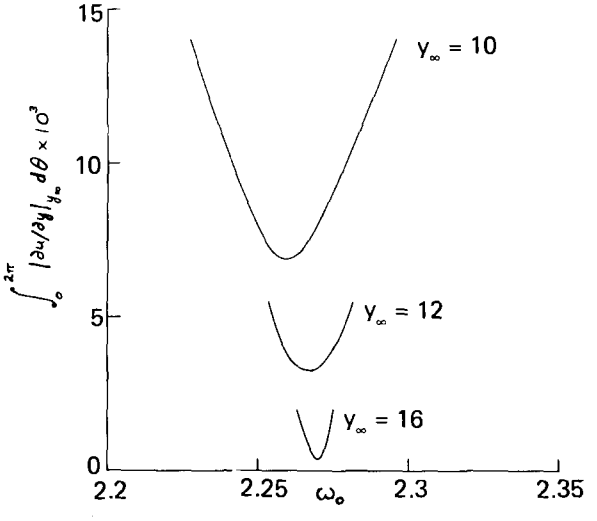

Figure 3. The vorticity measure at the edge of the boundary layer for the case $e = 0.71$.

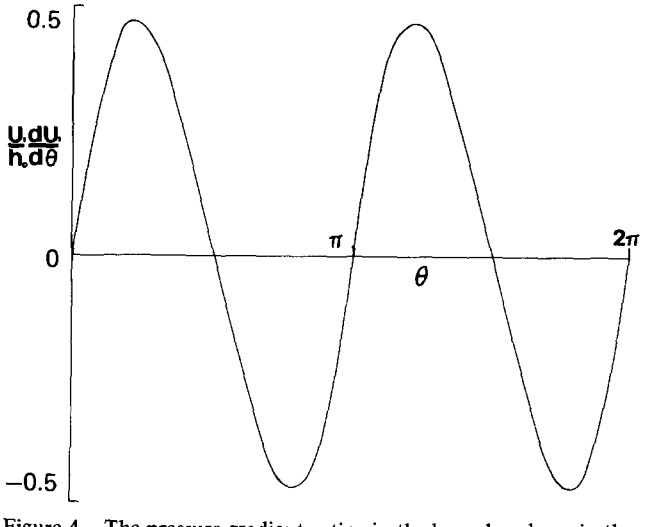

Figure 4. The pressure gradient acting in the boundary layer in the case $e = 0.77$.

In Figs 4 to 6 we show in more detail the results which we have obtained for $e = 0.77$ which, for the reasons discussed below, is the most eccentric of the ellipses that we are able to treat in this way. For this ellipse we have calculated $\omega_0 = 2.2911$, and in Fig. 4 we show the pressure gradient which is the forcing term in (3.11), and we see that in this case the boundary layer develops under substantial variations of pressure. In Fig. 5 we show U_s and U_1, where for the latter free-stream velocity we have also included the constant pressure result $e = 0$ for comparison. In the four parts of Fig. 6 we show velocity profiles at various stations in the boundary layer, and we include also those appropriate to $e = 0$ for comparison. There is nothing exceptional about these profiles, but we do note that the velocity variations within the boundary layer in the case $e = 0$ simply reflect the variations in U_s, since U_1 is constant. For the case $e = 0.77$ the velocity distribution is not only affected by the variations of U_s and U_1 but also by the pressure gradient which acts across the whole of the boundary layer, and the effect of this can be seen in the profiles. We have noted in our calculations that for slightly larger values of e the pressure gradient has an increasing effect upon the boundary layer, to the extent that although U_s and U_1 are always positive the pressure gradient reduces the velocity to zero at a point y_i where $0 < y_i < y_\infty$. When this first happens $\partial u/\partial y = 0$ also at $y = y_i$, and it is known from the work of Brown [4] that for boundary-layer flow under a prescribed pressure gradient a singularity develops whenever u and $\partial u/\partial y$ vanish simultaneously at an interior point. We have noted the development of such a singularity in our solution, which has precluded the possibility of us extending our results to higher values of e. We believe that this singular point anticipates a region of reversed flow, as in the case of classical boundary-layer separation, and for that reason we suggest that the inviscid solution (3.7) may then no longer be appropriate.

In Fig. 7 we summarize some of our results by displaying the values of ω_0 which we have

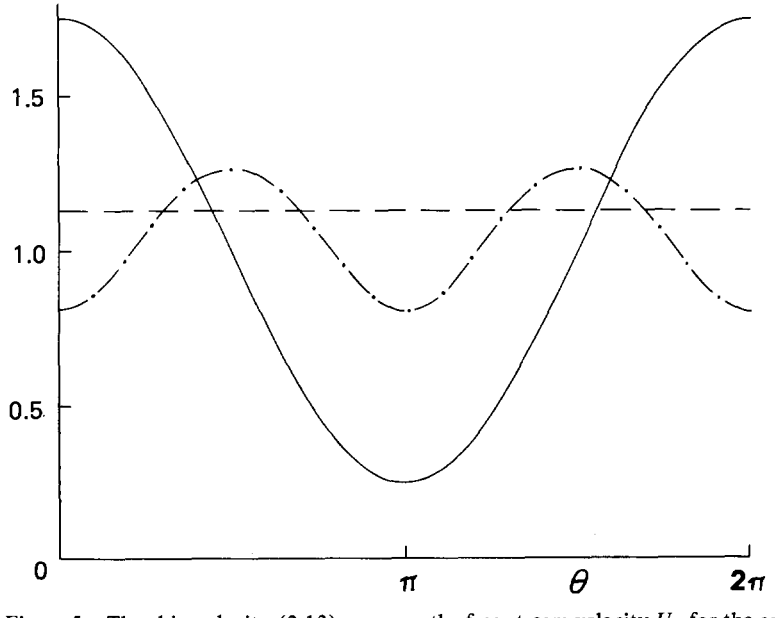

Figure 5. The skin velocity (3.13) ——— ; the free-stream velocity U_1 for the case $e = 0$ – – – – ; the free-stream velocity U_1 for the case $e = 0.77$ –·–·–·– .

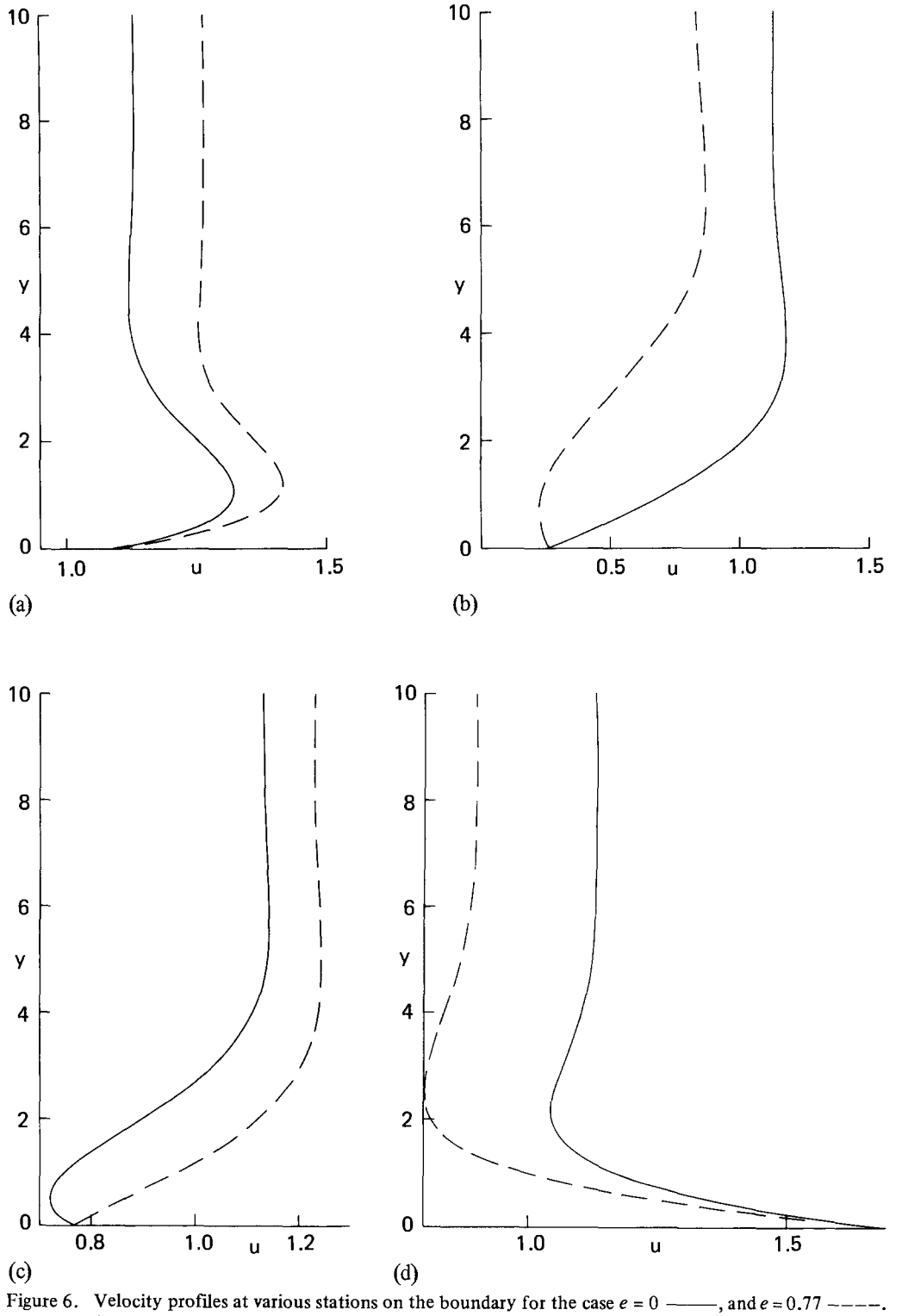

Figure 6. Velocity profiles at various stations on the boundary for the case $e = 0$ ——, and $e = 0.77$ – – – –. (a) $\theta = 7\pi/15$, (b) $\theta = 14\pi/15$, (c) $\theta = 21\pi/15$, (d) $\theta = 28\pi/15$.

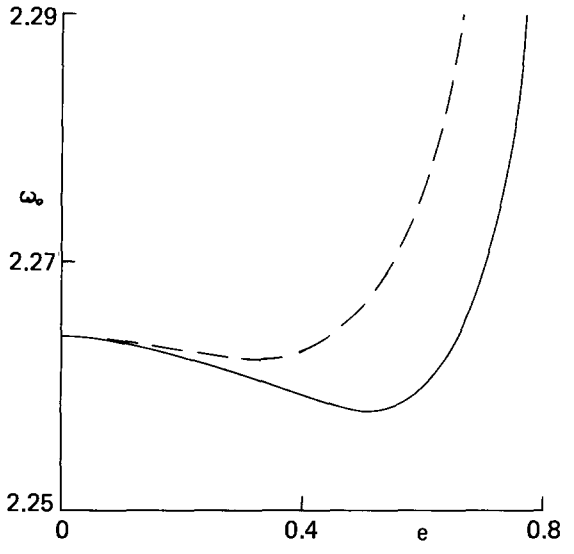

Figure 7. The core vorticity ω_0 for various values of e. The exact result ——— , equation (2.4) – – – –.

calculated for values of e up to $e = 0.77$. These have been obtained by carrying out the calculations described above on two mesh sizes and then using h^2-extrapolation. We also show in Fig. 7, for comparison, the values of ω_0 calculated by applying the result (2.4) to this case and note the reasonable agreement with the exact result. Burggraf [5], in his study of the square cavity problem via numerical solutions of the Navier-Stokes equations, has also noted that as the Reynolds number R increases the core vorticity becomes close to that which may be derived from the result (2.4). It seems not unreasonable therefore to conjecture that (2.4) will provide a sensible approximation to the core vorticity in most situations. It has been used in this way by, for example, Burggraf [5].

In conclusion we note that although the method which we have adopted enables us to determine the inviscid core vorticity accurately the calculations are quite lengthy. As a consequence it may be not significantly less economical to obtain numerical solutions from the Navier-Stokes equations at high Reynolds numbers as in [2], or the more recent work of Lewis [6]. From such calculations not only can the inviscid core vorticity be evaluated by extrapolation, but finite Reynolds number effects within the flow-field can also be assessed. Furthermore, regions of separated flow can be accommodated whereas the method of solution described in this paper, based upon the boundary-layer equations, may fail due to the development of singular behaviour.

REFERENCES

[1] G. K. Batchelor, On steady laminar flow with closed streamlines at large Reynolds number, *J. Fluid Mech.* 1 (1956) 177-190.

[2] O. R. Burggraf, Analytical and numerical studies of the structure of steady separated flows, *J. Fluid Mech.* 24 (1966) 113-151.

[3] E. G. Smith, Closed streamlines in boundary layers, M.Sc. Dissertation, Bristol University (1973).
[4] S. N. Brown, Singularities associated with separating boundary layers, *Phil. Trans. R. Soc. A* 257 (1965) 409-444.
[5] O. R. Burggraf, Computational study of supersonic flow over backward-facing steps at high Reynolds number, *Aero. Res. Lab. Rept. 70-0275* (1970).
[6] E. Lewis, Steady flow between a rotating circular cylinder and a fixed square cylinder, *J. Fluid Mech.* 95 (1979) 497-513.